

Equivalent Circuit Analysis of Serpentine Folded-waveguide Slow-wave Structures for Millimeter-wave Traveling-wave Tubes

M. Sumathy · K. J. Vinoy · S. K. Datta

Received: 27 June 2008 / Accepted: 26 September 2008 /
Published online: 1 November 2008
© Springer Science + Business Media, LLC 2008

Abstract A simple equivalent circuit model for the analysis of dispersion and interaction impedance characteristics of serpentine folded-waveguide slow-wave structure was developed by considering the straight and curved portions of structure supporting the dominant TE_{10} -mode of the rectangular waveguide. Expressions for the lumped capacitance and inductance per period of the slow-wave structure were derived in terms of the physical dimensions of the structure, incorporating the effects of the beam-hole in the lumped parameters. The lumped parameters were subsequently interpreted for obtaining the dispersion and interaction impedance characteristics of the structure. The analysis was simple yet accurate in predicting the dispersion and interaction impedance behaviour at millimeter-wave frequencies. The analysis was benchmarked against measurement as well as with 3D electromagnetic modeling using MAFIA for two typical slow-wave structures (one at the Ka-band and the other at the W-band) and close agreement observed.

Keywords Equivalent circuit analysis · Serpentine folded-waveguide (SFW) · Slow-wave structure (SWS) · Traveling-wave tube (TWT)

Abbreviations

SFW Serpentine Folded-waveguide
SWS Slow-wave structure
TWT Traveling-wave tube

M. Sumathy (✉) · S. K. Datta
Microwave Tube Research and Development Centre, Bharat Electronics Complex, Jalahalli Post,
Bangalore 560013, India
e-mail: msumti@yahoo.co.in

K. J. Vinoy
Department of Electronics & Communication Engineering, Indian Institute of Science, Bangalore
560054, India

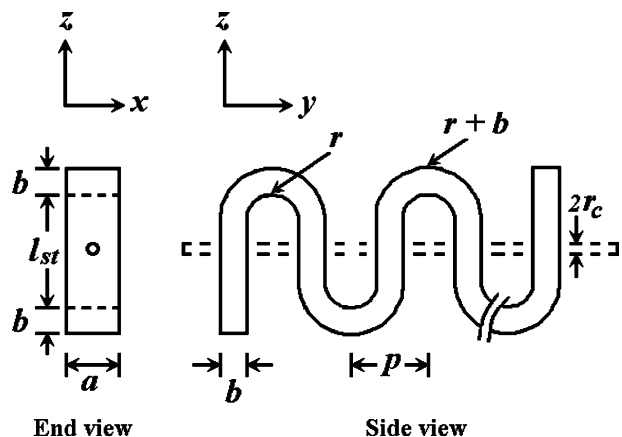
1 Introduction

The serpentine folded-waveguide traveling-wave tubes (TWTs) find applications at millimeter-wave frequencies due to its robust construction, high power capability, simpler coupling and reasonably wide bandwidth. Such a TWT uses a serpentine folded-waveguide slow-wave structure (Fig. 1) that belongs to the fundamentally backward class of circuits like that of a coupled-cavity slow-wave structure. The folded-waveguide slow-wave structure is preferred for millimeter-wave applications for the ease of mechanical fabrication due to its simple structural configuration.

A renewed interest is observed for this class of slow-wave structure [1–5] for millimeter-wave sources, where the design of the slow-wave structure has been carried out mainly through 3D electromagnetic modeling. However, analytical approaches, for the analysis of dispersion and interaction impedance characteristics of a serpentine folded-waveguide slow-wave structure, have been sparse in the published domain of literature. Only four approaches have been in vogue in this regard: the approaches from S. Liu [6], Na *et al.* [7], Han *et al.* [8] and Booske *et al.* [9]. Liu [6] proposed a simple analytical procedure based on empirical formulation to find out the dispersion and interaction impedance of a serpentine folded-waveguide slow-wave structure excluding the effect of the beam-hole. Subsequently, work of Han *et al.* also proposed an analytical approach ignoring the effect of the beam-hole [8]. A thorough equivalent circuit analysis of serpentine folded-waveguide slow-wave structure including the effect of the presence of the beam-hole was proposed both by Na *et al.* [7] and Booske *et al.* [9] for the calculation of dispersion characteristics following the approach of transmission line cascading network and benchmarked against 3D electromagnetic modeling using HFSS, MAFIA and Microwave Studio by Booske *et al.* [9] and using MAGIC and HFSS by Na *et al.* [7]. Both these approaches ignore the analysis and benchmarking of interaction impedance. However, analysis of both the dispersion and interaction impedance characteristics including the effect of beam-hole has not been fully developed and benchmarked in the published literature.

In the present work we propose a complete equivalent circuit model for a serpentine folded-waveguide slow-wave structure for the analysis of both dispersion and interaction impedance characteristics including the effect of the beam-hole. The analysis stems from the high pass filter model as proposed by Curnow [10] for arriving at the lumped circuit inductance and capacitance per period of the structure. These inductance and capacitance obtained from the equivalent circuit analysis are subsequently used to interpret the

Fig. 1 Schematic of a typical serpentine folded-waveguide slow-wave structure showing the relevant dimensions.



dispersion and interaction impedance of the structure for the forward space-harmonic mode. The analysis developed here has been benchmarked against measurement and 3D electromagnetic model using MAFIA with close agreement.

Further, the analytical model has been used to demonstrate the effects of dimensional variations on the dispersion and interaction impedance of the structure. Effects of the other dimensional variations, like *a*-dimension and *b*-dimensions, on both dispersion and interaction impedance have already been studied in the literature [6], [9]. Booske *et al.* [9] also studied the effect of beam-hole variation on the dispersion characteristics. However, as far as the authors are aware, the analysis and studies of the effect of beam-hole on the interaction impedance has not been reported so far. The present approach having the effect of beam-hole included in the formulation has been able to analyze its effect on the interaction impedance. It was observed that suitable control of the beam-hole diameter could improve the interaction impedance thereby opening a possibility of efficiency enhancement.

2 Analysis

The analysis stems from the consideration that each period of the serpentine folded-waveguide consists of two wave-guide elements: (1) a straight rectangular waveguide section (having broad-dimension *a* and narrow-dimension *b*) accommodating the beam-hole as apertures at the broad-wall, and (2) an E-plane waveguide bend having the inner- and outer-bend radii *r* and *r + b*, respectively (Fig. 1). The E-bend segment of the serpentine structure is essentially a truncated 180° sector of a coaxial-waveguide having two co-axial cylindrical surfaces at inner radius *r* and outer radius *r + b*. The coaxial waveguide generally supports transverse electromagnetic mode of propagation along its axis. However, as it is truncated by placing two metallic boundaries perpendicular to its axis separated by the broad-wall dimension (*a*) of the standard rectangular waveguide, the mode configuration supported in the bent-segment becomes equivalent to *TE*₁₀ mode in standard rectangular waveguide enabling proper mode transition from straight-to-bent-waveguide sections.

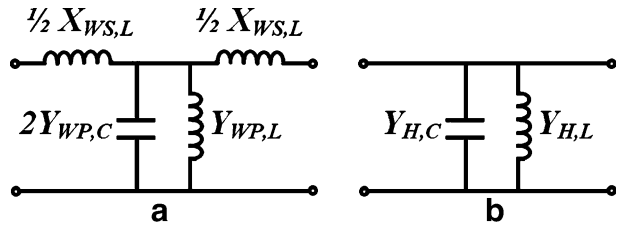
Thus, equivalent circuit modeling per period of the structure has been carried out in two parts. First we formulated the equivalent circuit parameters for the rectangular waveguide including the curved section supporting dominant *TE*₁₀ mode of propagation [11], and subsequently the equivalent circuit parameters for the beam-hole [9], and then coupled the parameters from both following Curnow’s approach [10].

In the absence of any loss in the circuit, a waveguide of unit length can be represented in terms of a series inductive reactance (*X*_{WS,L}), a shunt inductive susceptance (*Y*_{WP,L}) and a shunt capacitive susceptance (*Y*_{WP,C}) as shown in Fig. 2(a), which are used to obtain the lumped circuit elements as:

$$\begin{aligned}
 X_{WS,L} &= j\omega L_{WS} = j\omega \mu_0 \left(\frac{b}{a}\right) \\
 X_{WP,L} &= j\omega L_{WP} = \left(\frac{j\omega \mu_0}{k_{c,10}^2}\right) \left(\frac{b}{a}\right) \\
 X_{WP,C} &= \frac{1}{j\omega C_{WP}} = \left(\frac{1}{j\omega \epsilon_0}\right) \left(\frac{b}{a}\right)
 \end{aligned}
 \tag{1}$$

Here, ϵ_0 and μ_0 are permittivity and permeability of free space, respectively, and $k_{c,10}$ ($=\pi/a$) is the cut-off wave-number for the dominant *TE*₁₀ propagating mode in the waveguide. Distributed lumped circuit parameters, *L*_{WS} is the waveguide series inductance per unit length,

Fig. 2 Equivalent circuit representation of waveguide part alone (a), and each beam tunnel aperture (b).



L_{WP} is the waveguide shunt inductance per unit length and C_{WP} is the waveguide shunt capacitance per unit length. Equation (1) is further interpreted to yield the equivalent circuit parameters for the effective waveguide length per periodicity as:

$$\begin{aligned} L_{WS} &= \left(\frac{\mu_0 b}{a}\right) \times l_{eff} \\ L_{WP} &= \left(\frac{\mu_0 a b}{\pi^2}\right) \times l_{eff}, \\ C_{WP} &= \left(\frac{\epsilon_0 a}{b}\right) \times l_{eff} \end{aligned} \tag{2}$$

with l_{eff} as the effective length of the waveguide per period, expressed in terms of straight waveguide length (l_{st}) and length of the E-bend as:

$$l_{eff} = l_{st} + \pi \left(r + \frac{b}{2}\right). \tag{3}$$

The total equivalent shunt inductance (L_W) and shunt capacitance (C_W) for the waveguide part of the structure per period can now be expressed as:

$$L_W = \frac{\mu_0 l_{eff} b}{\pi^2 (l_{eff} + b)} \quad \text{and} \quad C_W = \epsilon_0 l_{eff} \frac{(l_{eff} + b)}{b}. \tag{4}$$

Next, one needs to consider the coupling of electromagnetic fields in the serpentine waveguide structure to the beam through the beam-hole. The beam-hole is considered as a circular aperture at the broad-wall of the rectangular waveguide centered at the location of electric field maxima, the diameter of the aperture ($2r_c$) being small enough to support non propagating mode at the operating frequency. Thus, we treated the aperture as a stub at the broad-wall [12], and the equivalent circuit parameters as shown in Fig. 2 (b) for each aperture are expressed as:

$$\begin{aligned} L_H &= \frac{\pi M \lambda_g}{\omega^2 \lambda_g^2 ab \left(1 - \frac{2\pi M}{\lambda_g^2 b}\right)} \\ C_H &= \frac{2\pi}{Y_0 \omega \lambda_g ab \left(\frac{1}{M} - \left(\frac{\pi}{a^2 b} + \frac{2.74}{2\pi r_c^2}\right)\right)}. \end{aligned} \tag{5}$$

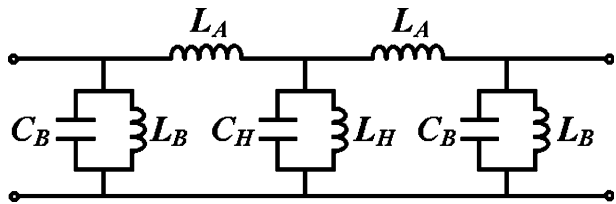
Here, Y_0 is the wave-admittance of the rectangular waveguide, λ_g is the guided-wavelength of the rectangular waveguide, and $M (= 8r_c^3/6)$ is an empirical factor [12].

Finally, one needs to cascade the two beam-hole apertures along with the waveguide as given in Fig. 3, which yields the equivalent circuit parameters for the structure per periodicity as follows:

$$L_A = \frac{2L_W}{k}, \quad L_B = \frac{2L_W}{1-k}, \quad \text{and} \quad C_B = 1/2 C_W, \tag{6}$$

with $k = \pi^2 r_c^2 (l_{eff} (a - p))^{-1}$.

Fig. 3 Equivalent circuit representation of one periodicity of the structure after cascading the waveguide and two beam-apertures.



Here, the coupling factor k is defined as the ratio of the beam tunnel surface area to the straight waveguide total surface area for a single periodicity of the slow-wave structure. Now, the task remains to express the dispersion relation following Curnow [10], in terms of the equivalent circuit parameters, expressed as:

$$\cos(\theta) = -\sqrt{\frac{Z_{OC}}{Z_{OC} - Z_{SC}}}. \tag{7}$$

Here, $\theta (= \beta p)$ is the total phase shift per periodicity of the structure. Z_{OC} and Z_{SC} are the input impedances of the circuit in Fig. 3 with its output open- and short-circuited, respectively, expressed as:

$$Z_{OC} = Z_B \frac{Z_A^2 + 2Z_A Z_H + Z_A Z_B + Z_B Z_H}{Z_A^2 + Z_B^2 + 2Z_A Z_B + 2Z_A Z_H + 2Z_B Z_H},$$

and

$$Z_{SC} = Z_B \frac{Z_A^2 + 2Z_A Z_H}{Z_A^2 + 2Z_A Z_H + Z_A Z_B + Z_B Z_H},$$

with

$$Z_A = \frac{2j\omega L_W}{k}, \quad Z_B = \frac{2j\omega L_W}{1 - k - \omega^2 L_W C_W} \quad \text{and} \quad Z_H = \frac{j\omega L_H}{1 - \omega^2 L_H C_H}.$$

Fig. 4 Dispersion and interaction impedance characteristics of the Ka-band structure and its benchmarking with measurement and MAFIA simulation. The structure uses a non-standard WR-28 waveguide having normalized dimensions $a/p=3.675$, $b/p=0.364$, $l_{st}/p=1.838$, $r/p=0.317$ and $r_c/p=0.165$.

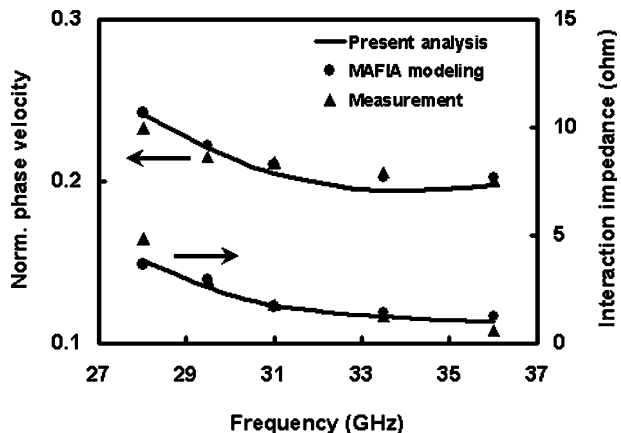
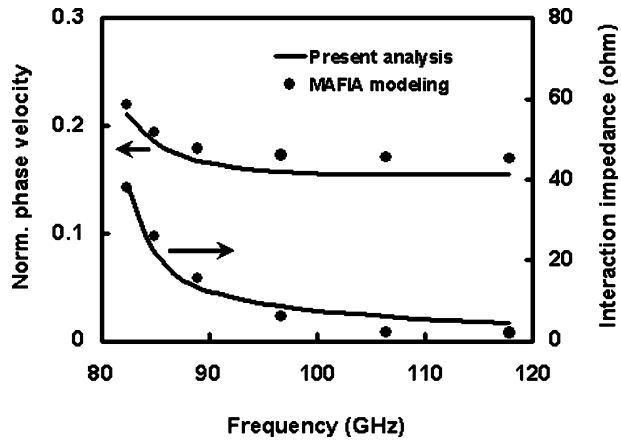


Fig. 5 Dispersion and interaction impedance characteristics of the W-band structure and its benchmarking with MAFIA simulation. The structure uses a non-standard WR-10 waveguide having normalized dimensions $a/p=4.625$, $b/p=0.45$, $l_{st}/p=2.313$, $r/p=0.313$ and $r_c/p=0.1$.



Equation (7) on simplification, yields,

$$\cos(\theta) = -1 - \frac{2Z_A}{Z_B} - \frac{Z_A}{Z_H} - \frac{Z_A^2}{Z_B Z_H},$$

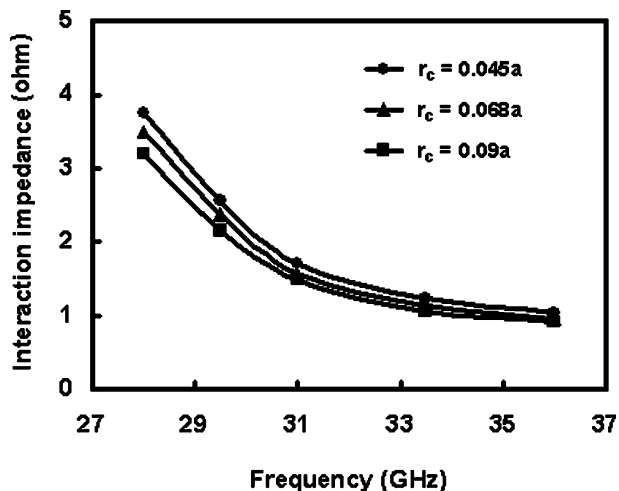
which on further simplification, yields the dispersion relation for the slow-wave structure, corresponding to the forward space-harmonic propagation mode, as:

$$\beta = \left(\frac{1}{p}\right) \cos^{-1} \left(1 - \left(\frac{L_W}{k^2 L_H}\right) \left\{ 1 - \omega^2 L_W C_W \right\} \left\{ 1 + \frac{2k L_H}{L_W} - \omega^2 L_H C_H \right\} \right), \quad (8)$$

Subsequently, using the dispersion relation (8), one can easily express the on-axis forward space-harmonic interaction impedance (K) of the slow-wave structure following Liu [6] and Carter [11] as:

$$K = \sqrt{\frac{L_W}{C_W}} \frac{1}{(\beta p)^2} \left(\left(1 - \left(\frac{1}{\omega \sqrt{L_W C_W}} \right)^2 \right)^{-\frac{1}{2}} \right) \left(\frac{\sin \beta b / 2}{\beta b / 2} \right)^2 \quad (9)$$

Fig. 6 Interaction impedance characteristics of the Ka-band structure with the beam-hole radius as the parameter.



Here, the parameters bear the meaning given in the text. The equations (8) and (9) may now be used for computing the dispersion and interaction impedance characteristics, respectively, with the knowledge of the dimensions of the structure under consideration.

3 Results and discussion

For numerical appreciation and benchmarking of the analysis, we considered two typical serpentine folded-waveguide structures, one operating at Ka-band frequency and the other at the W-band. The benchmarking of the analysis has been carried out for both the structures with respect to 3D electromagnetic modeling using MAFIA, while the analysis was further benchmarked against measurement only for the Ka-band structure. The Ka-band structure was fabricated using wire-EDM technique and specially designed couplers were joined to its ports for the measurement. The measurement on the Ka-band structure was carried out following standard non-resonant perturbation method [13]. The benchmarking results are presented in Fig. 4 and 5. The analytical results show excellent accuracy with the measurement and MAFIA simulated results.

Now it would be of interest to analyze the effect of beam-hole dimension on the interaction impedance characteristics of the structure. We carried out the study typically for the Ka-band structure (Fig. 6). It was observed that the increase in the beam-hole diameter accompanies a fall in the interaction impedance. One may, therefore, tailor the beam-hole radius for desired interaction impedance for optimum interaction efficiency.

4 Conclusion

Present work embodies a simple equivalent circuit analysis for the serpentine folded-waveguide slow-wave structures useful for millimeter-wave traveling wave tube. The approach is complete in the sense that it includes the effects of beam-hole for both dispersion and interaction impedance characteristics, which have not been available in reported literatures. It is expected that the simplicity and compactness of the approach along with thorough benchmarking for different millimeter-wave frequency band would be of ample use for the millimeter-wave community.

Acknowledgments The authors are thankful to Dr. Lalit Kumar, Dr. K. S. Bhat and Dr. V. Latha Christie for many valuable suggestions to improve the work. Authors are also thankful to Microwave Tube R&D Centre for kind permission to use the experimental results.

References

1. J. Cai, J. Feng, Y. Hu, X. Wu, B. Qu, S. Ma, J. Zhang, and T. Chen, Attenuator for W-band folded waveguide TWT. *Proceedings of the IEEE International Vacuum Electronics Conference 9th*, USA, 20–21 (2008).
2. H. –R. Gong, Y. –B. Gong, Z. –G. Lu, W. –X. Wang, and J. Feng, The design of Ka-band high power folded waveguide traveling-wave tube. *Proceedings of the IEEE International Vacuum Electronics Conference 9th*, USA, 119–120 (2008).
3. A. J. Thesis, C. J. Meadows, K. L. Montgomery, and M. Martin, Development of a high average power W-band TWT. *Proceedings of the IEEE International Vacuum Electronics Conference 9th*, USA, 197–198 (2008).

4. J. Feng, J. Cai, X. Wu, S. Ma, Y. Hu, and M. Huang, Design investigation of 10W W-band folded waveguide TWT. *Proceedings of the IEEE International Vacuum Electronics Conference 8th*, Japan, 77–78 (2007).
5. J. K. So, Y. M. Shin, K. H. Jang, J. H. Won, A. Srivastava, M. A. Sattarov, G. S. Park, J. H. Kim and S. S. Chang, Experimental study on 100 GHz two-step LIGA-based backward wave devices. *Proceedings of the IEEE International Vacuum Electronics Conference 8th*, Japan, 369–370 (2007).
6. L. Shunkang, Folded waveguide circuit for broadband MM wave TWTs. *Int. J. Infrared Millim. Waves* **16**, 809–815 (1995).
7. Y. H. Na, S. W. Chung, and J. J. Choi, Analysis of a broadband Q-band folded-waveguide traveling-wave tube. *IEEE Trans. Plasma Sci.* **30**, 1017–1022 (2002).
8. S. -T. Han, J. -II Kim, and G. S. Park, Design of a folded waveguide traveling-wave tube. *Microw. Opt. Technol. Lett.* **38**, 161–165 (2003).
9. J. H. Booske, M. C. Converse, C. L. Kory, C. T. Chevalier, D. A. Gallagher, K. E. Kreisler, V. O. Heinen, and S. Bhattacharjee, Accurate parametric modeling of folded waveguide circuits for millimeter-wave traveling wave tubes. *IEEE Trans. Electron Devices* **52**, 685–693 (2005).
10. H. J. Cumow, A general equivalent circuit for couple-cavity slow-wave structures. *IEEE Trans. Microw. Theory and Tech.* **13**, 671–675 (1965).
11. R. G. Carter, and L. Shunkang, Method for calculating the properties of coupled-cavity slow-wave structures from their dimensions. *IEE Proc.-H, Microw. Ant. and Prop.* **133**, 330–334 (1986).
12. N. Marcuvitz, *Waveguide Handbook*. (Peter Peregrinus, London, 1986).
13. M. Genack, S. Bhattacharjee, J. Booske, C. Kory, S. -J. Ho, D. van der Waide, L. Ives, and M. Read, Measurements of microwave electrical characteristics of folded waveguide circuits. *Proceedings of the IEEE International Vacuum Electronics Conference 5th*, USA, 2004, pp. 96–97.